Synthesis, Conformational Studies and Mannosidase Stability of a Mimic of 1,2-Mannobioside

Silvia Mari,[b] Helena Posteri,[a] Gilles Marcou,[a] Donatella Potenza,[a] Fabrizio Micheli,[c] F. Javier Cañada,[b] Jesus Jimenez-Barbero,*[b] and Anna Bernardi*[a]

Keywords: Carbohydrate mimics / Conformational analysis / Mannobioside

Dimethyl (1*S*,2*S*,4*S*,5*S*)-4-allyloxy-5-(α-mannosyloxy)cyclohexane-1,2-dicarboxylate (**3**) was designed as a structural mimic of α(1,2)mannobioside (**1**). Its synthesis and structural analysis by NMR spectroscopy and molecular modelling are described. The results show that **3**, like **1**, populates two low-energy conformations — stacked (*S*) and extended (*E*) — that are in fast dynamic equilibrium around the glycosidic linkage. Thus, the data confirm the expectation that the pseudo-disaccharide can be used as a structural mimic of mannobioside. The mannosidase stability of **3** was found to be significantly higher (sixfold) than that of natural mannobioside. This is a very useful feature of this mimic and is encouraging for its future development.

Introduction

During the past few years a number of publications and reviews have illustrated the potential of sugar mimics in different fields of drug discovery.[1−3] The main advantage of this approach is rooted in the improved drug-like character of glycomimetics compared to natural carbohydrates. Sugar mimics are generally more soluble and membrane penetrant, less hydrophilic and less metabolically labile than the sugars themselves.

Our groups are actively involved in the rational design and synthesis of glycomimetics based on the concept of scaffold replacement.[4] In brief, we have proposed the use of conformationally stable cyclic diols to replace the non-pharmacophoric parts of bioactive oligosaccharides, while preserving the correct orientation of the pharmacophoric portion of the sugar. Computational tools have been used to predict the three-dimensional structures of virtual mimic candidates and to compare them with the structure of the natural counterpart. This approach has been validated for a 3,4-disubstituted galactose scaffold (a *cis* diol) using the GM1:CT recognition pair as a model system.[5,6] Supported by appropriate experimental work,[7−10] molecular modelling has also allowed us to obtain qualitative predictions of the binding mode of the new substrates and to design further simplifications of glycomimetic structures. We now present our results relative to glycomimetics containing an analog of the αMan1,2-disubstituted framework (a *trans*-diaxial diol). A mimic of the 1,2-mannobioside **1** was prepared by replacing the reducing-end mannose unit with the carbocyclic diol **2** [(1*S*,2*S*,4*S*,5*S*)-dicarboxycyclohexane diol, DCCHD; Figure 1],[4] a conformationally stable 1,2 *trans*-diaxial diol.[4,11] Computer-aided molecular design (see below) suggested that **2** can be used as a mimic of the 2-substituted α-mannose unit in **1** without altering the overall shape of the molecule and therefore the presentation of the terminal (non-reducing end) residue. NMR studies confirmed that the resulting pseudo-mannobioside **3** has indeed the same conformational behavior as the natural disaccharide, but exhibits improved stability towards the activity of jack-bean mannosidase.

Synthesis of the Mannobioside Mimic 3

The enantiopure *trans*-diaxial DCCHD scaffold **5** (Scheme 1) was synthesized in 81% overall yield starting from the known diacid **4**[12] by *m*-chloroperbenzoic acid (MCPBA) double-bond oxidation, followed by $Cu(OTf)_2$-promoted opening of the epoxide with allyl alcohol.[4] The pseudo-disaccharide skeleton was then assembled by glycosylation of the acceptor **5** (Scheme 1) with tetraacetylmannose trichloroacetimidate (**6**).[13] The reaction was promoted by 0.25 molar equivalents of trimethylsilyl triflate (TMSOTf) in CH_2Cl_2 at −20 °C. At very short contact times (10 min) the orthoester **7** was initially formed by nu-

[a] Dipartimento di Chimica Organica e Industriale e Centro di Eccellenza CISI, Universita' di Milano
Via Venezian 21, 20133 Milano, Italy
Fax: (internat.) +39-02-503-14092
E-mail: anna.bernardi@unimi.it
[b] Departamento de Estructura y Funcion de Proteinas, Centro de Investigaciones Biologicas CSIC,
Ramiro de Maeztu 9, 28040 Madrid, Spain
Fax: (internat.) +34-91-536-0432
E-mail: jjbarbero@cib.csic.es
[c] GSK Medicine Research Centre
Via Fleming 4, 37135 Verona, Italy

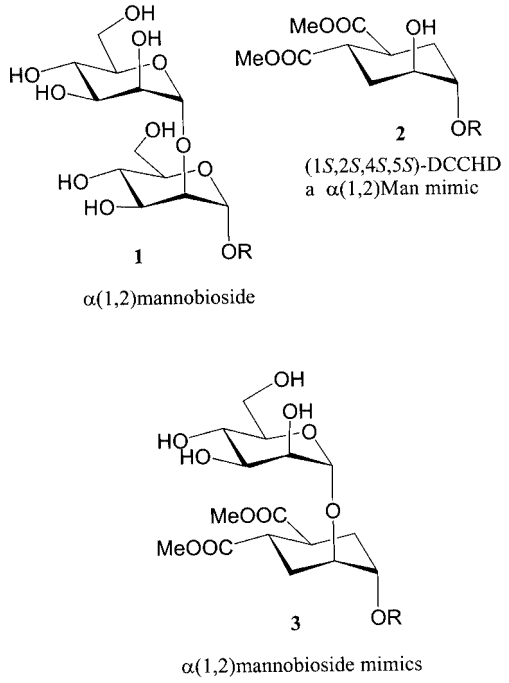

Figure 1. Mannobioside **1** and its DCCHD-based mimic **3**

cleophilic attack of **5** on the 2-acetate protecting group of **6**.[14] This product could be isolated by flash chromatography, and converted into **8** by treatment with TMSOTf in CH_2Cl_2 at −20 °C.[14] When allowing the reaction between **5** and **6** to stand for a somewhat longer time (20 min), the desired product **8** was obtained directly in 65% yield, after chromatography. Deacetylation (NaOMe in MeOH) quantitatively afforded **3**, whose structure was unequivocally confirmed by ^1H and ^{13}C NMR spectroscopy and by mass spectrometry.

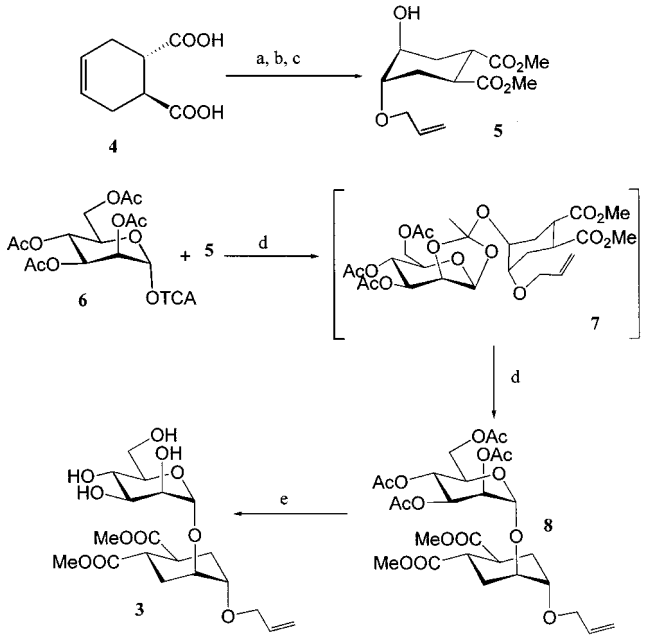

Scheme 1. Synthesis of the pseudo-mannobioside **3**: (a) MeOH, cat. H_2SO_4 (95%); (b) MCPBA, CH_2Cl_2 (95%); (c) allyl alcohol, 10% $Cu(OTf)_2$ (90%); (d) 25% TMSOTf, CH_2Cl_2, −20 °C (65%); (e) NaOMe, MeOH (88%)

Conformational Analysis of the Mannobioside Mimic 3

The conformation and dynamics of the Manα1-2-Man linkage were studied extensively in the oligomannose oligosaccharide $Man_9GlcNAc_2$.[15] Computational[15,16] and experimental[17] results suggested that the linkage exists in two distinct, flexible conformations with similar φ values and different, slowly interconvertings ψ values. The two conformations, which have been termed *S*, for "stacked", and *E*, for "extended", (Figure 2) are both represented in available X-ray structures of mannose oligosaccharides and account for the set of four NOE contacts typically observed across the glycosidic linkage.[17] The H1-H1′ contact (Figure 2) can arise from conformer *S*, and the H5-H1′ and H1-H3′ contacts (Figure 2) from conformer *E*. The fourth observed NOE contact belongs to the interglycosidic H1-H2′ pair, which is at NOE distance in both conformations. (The mutually exclusive NOE contacts are marked by arrows in Figure 2).

We recently reported[16] that modeling of **1** using the AMBER* force field and GB/SA solvation model gives results that are fully compatible with previous simulations and available experimental data. Two conformers, *S* (global minimum) and *E* (+6 kJ/mol), were located by an MC/EM conformational search, and were found to be freely interconverting and almost equally populated by MC/SD dynamic simulations. The same approach was then used to predict the three-dimensional structure of the 1,2-α-mannobioside mimic **3**; the molecule was calculated to populate the same region of conformational space as **1**. These results are presented in Figure 3. The unconventional numbering of the DCCHD ring shown in Figure 3 is used to facilitate comparison with **1**. An MC/EM conformational search of **3** located the *S* (φ = 94°, ψ = −72°; see c in Figure 3) and *E* (φ = 70°, ψ = −117°; see d in Figure 3) conformers at +2.6 kJ/mol and 0.0 kJ/mol relative energy, respectively. The dynamic simulation (10 ns, see b in Figure 3) showed that the two conformations are in fast dynamic equilibrium around the glycosidic linkage. Compared to **1**, the conformational space available to **3** is more biased towards the region populated by extended (*E*) conformations. Furthermore, the *E* region of the conformational space appears broad and is not centered around its local minimum at φ = 70°, ψ = −117°, but rather around larger values of ψ. This can clearly be seen in the map of Figure 3, and has important consequences on the calculated interproton distances, some of which display a strong dependence on the value of the ψ torsion (cf the distances calculated by the MC/SD dynamics with those of the isolated minima in Table 1). In summary, computer-aided molecular design clearly supports the expectation that the pseudo-disaccharide **3** can be used as a structural mimic of mannobioside **1**.

NOESY data were collected at 400 MHz for **3** in D_2O solution at 25 °C (Table 1, column 1) and compared with the MC/SD simulation predictions. A qualitative analysis

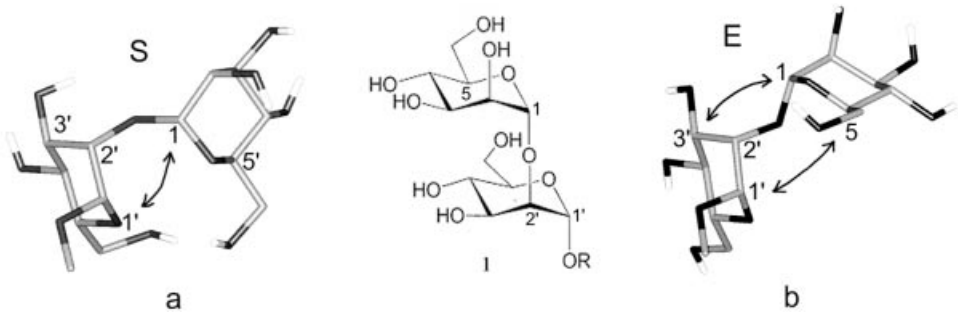

Figure 2. Low-energy conformations of the 1,2-mannobioside **1**: (a) the stacked conformation *S* ($\Phi = 88°$, $\Psi = -58°$); (b) the extended conformation *E* ($\Phi = 72°$, $\Psi = -138°$); characteristic NOE contacts are indicated by arrows

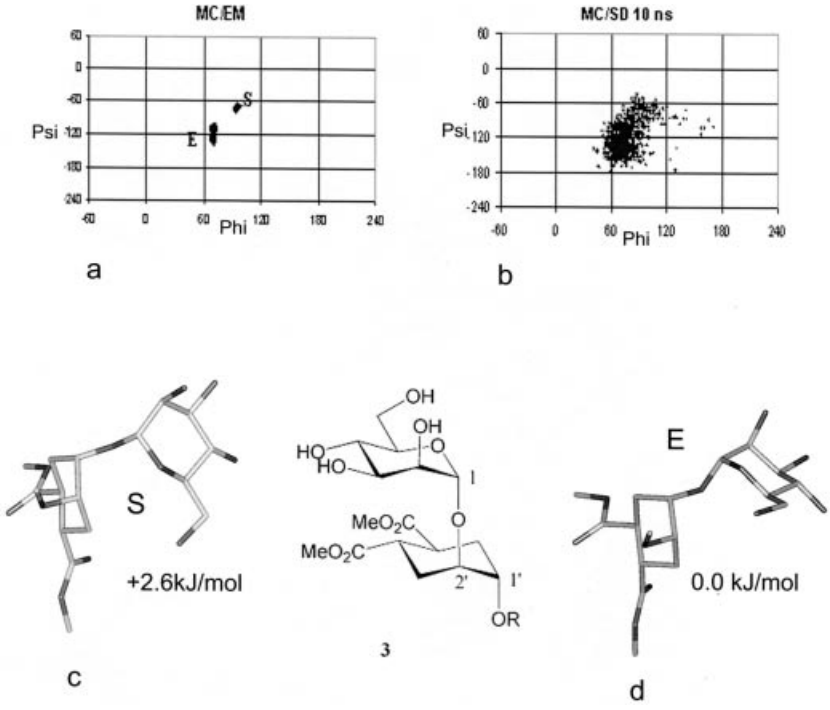

Figure 3. Conformational studies on pseudo 1,2-α-mannobioside **3** (MMOD 5.5, AMBER*, GB/SA water solvation); an unconventional numbering of the DCCHD moiety is used to help comparison with 1,2-mannobioside. Φ: O5−C1−O1-C2′; Ψ: C1−O1−C2′−C1′; (a) 10000 steps of MC/EM conformational search; (b) 10 ns of MC/SD dynamic simulation; (c) conformer *S* ($\Delta E = 2.6$ kJ/mol; $\Phi = 94°$, $\Psi = -72°$); (d) the lowest energy conformation *E* ($\Phi = 70°$, $\Psi = -117°$)

Table 1. Interresidue NOE contacts observed in the D_2O spectrum of **3**

Proton pair[a]	NOE intensity[b] (D_2O)	Calcd. distance (Å)[c]	Calcd. distance *E* (Å)	Calcd. distance *S* (Å)	Exp. distance range in **1** (Å)[d]
H1-H1′	w	3.4	3.9	2.6	2.9−3.0
H1-H2′	s	2.3	2.2	2.2	2.1−2.2
H1-H4′	w	3.8	4.2	4.6	no NOE
H1-H3′ax	−	4.0	4.1	4.5	3.2−3.6
H1-H3′eq	s	2.7	3.0	4.0	−
H2-H4′	m	3.7	4.0	4.8	n.r.[e]
H5-H2′	m	3.4	3.6	3.6	n.r.[e]
H5-H1′	s	2.6	2.3	4.4	2.5−2.7
H5-H6′ax	m	2.8	2.9	2.2	−
H5-H4′	w	4.2	4.5	3.2	n.r.[e]

[a] Numbering as in Figures 2 and 3. [b] s: strong, m: medium, w: weak. [c] Evaluated from $<r^{-6}>$ monitored during 10 ns of the MC/SD simulation. [d] From ref.[15] [e] Not reported.

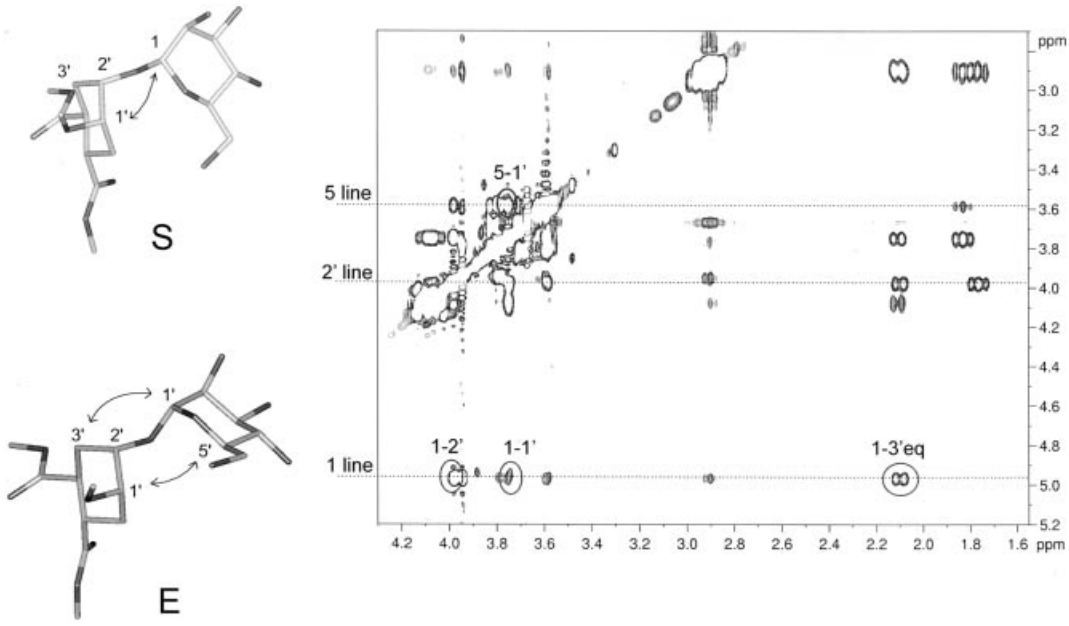

Figure 4. NOESY spectrum of mimic **3** in D_2O at 400 MHz (25 °C) with a mixing time of 800 ms; exclusive *S* and *E* conformation NOE contacts (indicated by the arrows) are found in the spectrum (circles), thus confirming that both the predicted conformations coexist

of the NOE crosspeaks using a basic strong-medium-weak intensity approach allowed us to deduce the presence of both *E* and *S* conformers in fast conformational equilibrium. Both sets of mutually exclusive NOE contacts were found in the spectra — the H1-H1′ contact originating from the *S* conformers, and the H1-H3′ and H5-H1′ contacts originating from the *E* conformers (Figure 4).

Despite this qualitative approach, we could safely deduce that the *E* conformer is the major one in solution, given the strong differences between the intensities of the corresponding NOE cross-peaks. Indeed, the observed correlations are in excellent agreement with the simulations (Table 1).

Compared to the experimental data range reported for the equivalent distances in **1**[15] (Table 1, last column), our data confirm that the conformational space of pseudo-mannobioside **3** is biased towards the extended conformation region. This is clearly shown by the weak intensity of the H1-H1′ cross-peak (Table 1, entry 1, and Figure 4, inset of the NOESY spectrum), a reporter signal of conformer *S* (Figure 4, *S*), which is much stronger in **1** than in **3**. Furthermore, the strong interaction observed in the NOESY spectrum of **3** for the H5-H1′ pair (Table 1, entry 8) is typical of extended conformations (Figure 4, *E*). This picture is also supported by the intense H1-H3′eq cross-peak (Table 1, entry 5, and Figure 4) and by the presence of a medium intensity H2-H4′ NOE contact (Table 1, entry 6), which is not seen in **1**. This latter contact could not be explained by the calculated structure of the *E* local minimum (Table 1, Column 3), but is in good agreement with the results of the dynamic simulation (Table 1, Column 1) and is an indication that the dynamic behavior of the molecule is well reproduced by the AMBER* calculations.

Thus, the NMR studies experimentally support the computational hypothesis that **3** behaves as a structural mimic of mannobioside, and preferentially populates the extended (*E*) conformation.

Mannosidase Stability of 3

The stability of **3** to mannosidase-catalyzed hydrolysis was investigated by submitting it to hydrolytic conditions in the presence of commercial jack-bean mannosidase. The substrate was incubated with increasing concentrations of the enzyme at pH 4.5 (maximum activity pH for α-mannosidases).[18] After 30 min of incubation at 37 °C the reaction mixture was lyophilized and the products were analyzed by GC. The extent of hydrolysis was evaluated by integration of the peaks relative to **3** (retention time, t_R, of 13.5 min) and to the aglycon **5** (t_R = 7.1 min). At the lowest enzyme concentration (0.5 μg/mL) 4% hydrolysis of mimic **3** was revealed by GC analysis, while, upon increasing the enzyme concentration up to 10 μg/mL, only 10% hydrolysis was observed. Under the same conditions 24% of the natural disaccharide **1** is already hydrolysed at an enzyme concentration of 0.5 μg/mL and 60% is hydrolysed at 10 μg/mL enzyme concentration. Thus, **3** indeed appears to be a substrate of jack-bean mannosidase, but it appears to be significantly more stable than **1** to the action of the enzyme. These observations prompted us to examine the ability of **3** to perform as an inhibitor for this enzyme.

Investigation of **3** as a possible inhibitor of mannosidase activity was carried out using α-mannosidase from jack-bean and *p*-nitrophenol-α-D-mannoside (PNP-Man) as the substrate (Table 2). The enzymatic reactions were run at 25 °C for 20 min and then quenched by adding a 1 M carbonate solution until pH 12, which inactivates the enzyme. The extent of the reaction was calculated from the absorbance of *p*-nitrophenoxide measured at a wavelength of 400 nm ($\varepsilon_{400} = 1.77 \times 10^4\ M^{-1}cm^{-1}$). The concentration of *p*-nitro-

phenoxide versus concentration of substrate in the reaction volume was plotted and fitted to the Michaelis−Menten equation to give a K_M value of 4.7×10^{-3} M, which is similar to the reported value of 2.5×10^{-3} M.[18] Qualitative inhibition studies were then performed using **3** as inhibitor and working with an enzyme concentration of 2.5 μg/mL (Table 2). The inhibitory effect of **3** allows us to estimate an average value for the inhibition constant, K_i, of 1.0×10^{-2} M, assuming a competitive inhibitor model (Table 2). The K_i values obtained are similar to those reported in the literature[18] for the known inhibitors mannono (1→4) and (1→5) lactone (1.0×10^{-2} M and 1.2×10^{-4} M, respectively).

Table 2. Inhibition of jack-bean-mannosidase-catalyzed hydrolysis of PNP-Man using **3**. The inhibition experiments were carried out for 20 min at 25 °C using 1.8 mM PNP-Man in citrate buffer (pH 4.5), a constant concentration of the enzyme (2.5 μg/mL) and variable concentrations of the inhibitor **3**. The reaction was quenched at pH 12 carbonate buffer and the concentration of the *p*-nitrophenoxide [PNP] was measured by UV spectroscopy. v_0 (0.025 mM/min) was obtained under the same conditions but in the absence of **3**.

[**3**] (mM)	[PNP] (mM)	$v_{Inhibited}$ (mM/min)	v_I/v_0	K_i[a] (mM)
12.8	0.28	0.014	0.565	11.9
10.1	0.31	0.015	0.626	12.3
5.1	0.32	0.016	0.651	6.8
2.5	0.41	0.021	0.841	9.7

[a] $$Ki = \frac{[I]\cdot K_M}{\frac{K_M + [S]}{v_i / v_0} - K_M - [S]},$$

where K_M = 4.67 mM, [I] = [**3**] and [S] = [PNP-Man].

Discussion and Conclusions

The results presented here show that the enantiopure *trans*-diaxial diol scaffold **5** can be used as a replacement for a 1,2-disubstituted α-mannose residue to give, in a facile and high-yielding synthetic sequence, a pseudo-mannobioside **3** which shows a high structural similarity with the natural α-1,2-mannobioside. The conformational analysis of **3** performed by NMR spectroscopy and supported by computational modelling reveals that **3**, like **1**, populates two low-energy conformations *S* (stacked) and *E* (extended) that are in fast dynamic equilibrium. Relative to the natural counterpart, the conformational space available to the pseudo-disaccharide appears to be biased toward the *E* region.

The α-1,2-mannobioside is the recognized epitope in various important sugar-protein complexes.[19] Appropriate epitope presentation is a key factor in determining ligand affinity to carbohydrate-binding proteins. For instance, it has been shown recently that, although sialic acid and galactose, per se, interact weakly with the cholera toxin (with millimolar dissociation constants), when appropriately presented on three-dimensionally well-defined structures, such as the GM1 ganglioside[20] or appropriate structural mimics,[5] they give rise to tight complexes with dissociation constants in the nanomolar range. The structural similarity of **3** with the natural disaccharide **1** is therefore an important element that depends critically on the nature of the dicarboxycyclohexanediol aglycon chosen to mimic the reducing-end mannose. The mimic **3** could thus be introduced into more complex oligosaccharidic structures, preserving epitope presentation, while imparting metabolic stability to the synthetic construct. Furthermore, the structure of **3** allows easy conjugation to polyvalent aglycons, using either the carboxy groups or the ether substituent. The conformational behaviour of mimic **3** that we describe here could have useful implications in recognition events where the *E* conformation of the 1,2-mannobioside is selectively recognized by the receptor.

An increased stability to enzymatic degradation is often cited as one of the advantages of glycomimetics over natural oligosaccharides in the development of drugs. The stability of **3** to mannosidase-catalyzed hydrolysis appears, indeed, to be significantly higher than the stability of the natural compound **1**. This is a very useful feature of this mimic and is very encouraging for the future developments of DCCHD-based glycomimetic drugs.

Experimental Section

NMR spectra were recorded at 25−30 °C on Bruker AVANCE 400 and 500 MHz spectrometers. The cyclohexanediol moiety is numbered as in Figure 3. Chemical shifts ^1H and ^{13}C NMR spectra are expressed in ppm relative to TMS or to DSS for spectra recorded in D_2O. The NOESY spectra of **3** were recorded with mixing times of 400, 600 and 800 ms. Mass spectrometry was performed with a VG 7070 EQ-HF apparatus (FAB ionization), an Omniflex apparatus (MALDI ionization) or an Apex II ICR FTMS (ESI ionization). Optical rotations $[\alpha]_D$ were measured in a 1-dm path-length cell with 1 mL capacity on a Perkin−Elmer 241 polarimeter. Thin layer chromatography (TLC) was carried out with precoated Merck F_{254} silica gel plates. Flash chromatography (FC) was carried out with Macherey−Nagel silica gel 60 (230−400 mesh). Solvents were dried by standard procedures and reactions requiring anhydrous conditions were run under nitrogen. The diacid **4**[12] and the trichloroacetimmidate **6**[13] were prepared by published procedures.

Synthesis of Dimethyl (1*S*,2*S*,4*S*,5*S*)-4-Allyloxy-5-hydroxycyclohexane-1,2-dicarboxylate (5): H_2SO_4 (0.5 mL, 0.009mol) was added to a solution of the diacid **4**[12] (7.02 g, 0.041mol) in dry MeOH (100 mL). The solution was stirred at reflux for about 20 h and then concentrated under vacuum to about half of the original volume. EtOAc was added, the organic phase was washed with saturated $NaHCO_3$ and dried with Na_2SO_4 and the solvent was evaporated under reduced pressure to give dimethyl (1*S*,2*S*)-cyclohex-4-ene-1,2-dicarboxylate in 95% yield. An analytical sample was purified by flash chromatography: $[\alpha]_D$ = +127.3 (*c* = 1.23, $CHCl_3$). ^1H NMR (200 MHz, $CDCl_3$, 25 °C): δ = 2.6−2.1 (m, 4 H, CH_2), 2.85 (m, 2 H, H^1, H^2), 3.7 (s, 6 H, OCH_3), 5.7 (m, 2 H, H^4, H^5) ppm. ^{13}C NMR (53.3 MHz, $CDCl_3$, 25 °C): δ = 24.5, 40.96, 51.45, 124.66, 174.79 ppm.

The crude reaction product was then sumbitted to epoxidation conditions. Thus, MCPBA (1.85 g, 7.6 mmol) was added to a solution of the diester (1.5 g, 5.5 mmol) in CH_2Cl_2 (13 mL). The solution was stirred at room temperature for 3 h and the organic phase was washed with saturated $NaHCO_3$, dried and the solvents evaporated under reduced pressure. The crude was purified by flash chromatography on silica gel (hexane/EtOAc, 85:15) to yield the epoxide in 95% yield. $[\alpha]_D = +71.6$ ($c = 1.27$, $CHCl_3$). ^{1}H NMR (200 MHz, C_6D_6, 25 °C): $\delta = 1.55$ (ddd, $J = 15$, $J = 11$, $J = 2.3$ Hz, 1 H), 1.95 (m, 2 H), 2.30 (ddd, $J = 15$, $J = 4$, $J = 2$ Hz, 1 H), 2.55 (m, 1 H), 2.65 (m, 1 H), 2.75 (m, 1 H), 3.10 (ddd, $J = 11$, $J = 11$, $J = 4.6$ Hz, 1 H), 3.28 (s, 3 H), 3.30 (s, 3 H) ppm.

The catalyst $Cu(OTf)_2$ (0.07 mmol) was added to a solution of the epoxide (150 mg, 0.7 mmol) in allyl alcohol (1.5 mL, 2.2 mmol). The reaction mixture was stirred for 3 h at room temperature, whilst monitoring by TLC (hexane/EtOAc, 6:4). After completion of the reaction a saturated solution of NH_4Cl and NH_3 was added and the mixture was extracted with EtOAc. The organic layer was dried and the solvents evaporated under reduced pressure. The crude mixture was purified by flash chromatography on silica gel (hexane/EtOAc, 1:1) to give **5** in 90% yield. ^{1}H NMR (200 MHz, C_6D_6, 25 °C): $\delta = 2.05$ (m, 5 H), 2.52 (br. s, 1 H, exch), 3.40 (m, 9 H), 3.70−4.00 (m, 4 H), 5.15 (m, 2 H), 5.80 (m, 1 H) ppm. ^{13}C NMR (75 MHz, $CDCl_3$, 25 °C): $\delta = 27.0$, 30.6, 39.0, 39.4, 51.9, 67.3, 69.8, 75.9, 116.9, 134.8, 175.0 ppm. MS (FAB+): $m/z = 273$ [M + H$^+$].

Mannosylation of 5. Synthesis of 8: Ground 4-Å molecular sieves were added to a solution of **5** (493 mg, 1.81 mmol) and **6**[13] (1.33 g, 2.71 mmol) and the mixture was dried in vacuo overnight. Dry CH_2Cl_2 (50 mL) was then added under N_2 and the solution was stirred for about 15 min. The temperature was then adjusted to −20 °C and TMSOTf (63 μL, 0.724 mmol) was added. The solution was stirred at −20 °C for about 10 min, until TLC revealed the disappearance of **5** (hexane/EtOAc, 6:4). The reaction was neutralized by adding triethylamine and concentrated. The molecular sieves were then removed by filtration and the product was isolated by flash chromatography (hexane/EtOAc, 6:4), and purified a second time by chromatography ($CHCl_3$/acetone, 95:5), to give the orthoester **7** in 86% yield. $[\alpha]_D = +47$ ($c = 1$, $CHCl_3$). ^{1}H NMR (400 MHz, $CDCl_3$, 25 °C): $\delta = 1.75$ (s, 3 H, CH_3), 1.8−1.99 (m, 4 H, H^{3Dax,eq}), 2.2−2.15 (m, H^9, $COCH_3$), 2.95−3 (m, 2 H, H^{4D}, H^{5D}), 3.51 (d, 1 H, H^{1D}), 3.69 (s, 3 H, OCH_3), 3.7 (s, 3 H, OCH_3), 3.71 (m, 1 H, H^{5D}), 3.89 (m, 1 H, H^{2D}), 3.92 (dd, $J = 12$, $J = 5$ Hz, 1 H, H^{7a}), 4.09 (dd, $J = 12$, $J = 6$ Hz, 1 H, H^{7b}), 4.11 (dd, $J = 12$, $J = 5$ Hz, 1 H, H^{6a}), 4.28 (dd, $J = 12$, $J = 2.5$ Hz, 1 H, H^{6b}), 4.6 (m, 1 H, H^2), 5.12−5.31 (m, 2 H, H^9), 5.19 (s, 1 H, H^3), 5.25 (s, 1 H, H^4), 5.45 (d, $J = 2$ Hz, 1 H, H^1), 5.8−6.0 (m, 1 H, H^8) ppm. ^{13}C-HETCOR (100.6 MHz, $CDCl_3$, 25 °C): $\delta = 34$, 35, 40, 62.5, 66, 69, 70.5, 71, 73, 75, 77.5, 98, 117, 135 ppm. MS (FAB+): $m/z = 603$ [M + H$^+$].

Rearrangement of the orthoester was achieved by adding TMSOTf (0.65 μL, 0.0035 mmol), to a cold (−20 °C) solution of the orthoester **7** (21.3 mg, 0.035 mmol) in CH_2Cl_2 (600 μL). The mixture was stirred under nitrogen whilst monitoring by TLC ($CHCl_3$/acetone, 95:5). After 10 min the reaction was complete. The mixture was then treated with triethylamine and the solvents evaporated under reduced pressure. The residue was purified by flash chromatography on silica gel ($CHCl_3$/acetone, 97:3) to give **8** in 50% yield**.** The same product was also obtained in 65% yield by running the mannosylation of **5** with **6** at −20 °C for 20 min, and monitoring the conversion of **7** by TLC ($CHCl_3$/acetone, 95:5). $[\alpha]_D = +38$ ($c = 1.26$, $CHCl_3$). ^{1}H NMR (400 MHz, C_6D_6, 25 °C): $\delta = 1.74$ (s, 3 H, $COCH_3$), 1.77 (s, 3 H, $COCH_3$), 1.81 (s, 3 H, $COCH_3$), 1.85 (s, 3 H, $COCH_3$), 2.04−2.17 (m, 4 H, H^{3D}, H^{6D}), 3.3−3.5 (m, 2 H, H^{4D}, H^{5D}), 3.40 (s, 3 H, OCH_3), 3.46 (s, 3 H, OCH_3), 3.57 (m, 1 H, H^{1D}), 3.85 (dd, $J = 13$, $J = 6$ Hz, 1 H, H^{7a}), 3.95 (m, 2 H, H^{7b}, H^{2D}), 4.34 (m, 1 H, H^5), 4.37 (dd, $J = 12$, $J = 8$ Hz, 1 H, H^{6a}), 4.49 (dd, $J = 12$, $J = 6$ Hz, 1 H, H^{6b}), 5.11 (dd, $J = 9.2$, $J = 1.5$ Hz, 1 H, H^{9a}), 5.15 (d, $J = 1.5$ Hz, 1 H, H^1), 5.27 (dd, $J = 16$, $J = 1.5$ Hz, 1 H, H^{9b}), 5.65 (dd, $J = 3$, $J = 2$ Hz, 1 H, H^2), 5.8 (t, $J = 9.7$ Hz, 1 H, H^4), 5.82−5.91 (m, 2 H, H^3, H^8) ppm. ^{13}C-HETCOR (100.6 MHz, C_6D_6, 25 °C): $\delta = 28.5$, 52, 63, 70, 71, 72, 73, 75, 96, 118 ppm. MALDI-TOF: $m/z = 625.45$ [M + Na$^+$].

Synthesis of the Pseudo-1,2-α-mannobioside 3: 1 M Methanolic sodium methoxide (398 μL, 0.398 mmol) was added to a solution of **8** (120 mg, 0.199 mmol) in MeOH (20 mL) and stirring was continued at room temperature for 18 h. The reaction was monitored by TLC ($CHCl_3$/MeOH/H_2O, 60:35:5). Amberlite IR-120 was then added, the resin was removed by filtration and the solution was concentrated. The residue was purified by flash chromatography ($CHCl_3$/MeOH, 9:1), to give **3** in 88% yield. $[\alpha]_D = +58.2$ ($c = 1$, CH_3OH). ^{1}H NMR (500 MHz, D_2O, 25 °C): $\delta = 1.75$ (m, 1 H, H^{3Dax}), 1.82 (m, 1 H, H^{6Dax}), 2.09 (m, 2 H, H^{3Deq}, H^{6Deq}), 2.88 (dt, $J = 11.5$, $J = 3.4$ Hz, 2 H, H^{4D}, H^{5D}), 3.57 (m, 1 H, H^5), 3.58 (m, 1 H, H^4), 3.65 (s, 3 H, OCH_3), 3.66 (s, 3 H, OCH_3), 3.68 (m, 1 H, H^{6b}), 3.74 (q, $J = 3$ Hz, 1 H, H^{1D}), 3.77 (q, $J = 3.4$ Hz, 1 H, H^3), 3.79 (m, 1 H, H^{6a}), 3.94 (dd, $J = 3.4$, $J = 1.8$ Hz, 1 H, H^2), 3.97 (q, $J = 3$ Hz, 1 H, H^{2D}), 4.03 (m, 1 H, CH_2Oallyl), 4.09 (m, 1 H, CH_2Oallyl), 4.95 (d, $J = 1.8$ Hz, 1 H, H^1), 5.20 (m, 1 H, CH_2=), 5.29 (m, 1 H, CH_2=), 591 (m, 1 H, CH=) ppm.^{13}C NMR (125 MHz, D_2O, 25 °C): $\delta = 27$, 39.2, 52.6, 61.05, 66.9, 70, 70.5, 70.6, 70.7, 73.5, 73.7, 98.7, 118.3, 134.2 ppm. MS (FAB$^+$): $m/z = 457$ [M + Na$^+$]. HRMS (ESI$^+$) for $C_{19}H_{30}O_{11}Na^+$: calcd. 457.16803; found 457.16586.

Enzymatic Studies: Mannosidase stability assays were performed in 20 μL samples of 5 mM substrate (**3** or **1**) in pH 4.5 0.1 M phosphate-citrate buffer at 37 °C. Substrates were submitted to increasing concentrations of jack-bean mannosidase. Three enzymatic reactions were run, with 0.5, 2.5 and 10 μg protein/mL solutions prepared from stock commercial enzyme suspension (Sigma-M7257, 5 mg/mL). After 30 min incubation the crude mixtures were frozen and freeze-dried. In all cases lyophilized samples were completely trimethylsilylated by treatment with trimethylsilylimidazole and pyridine at 60 °C for 30 min, and were then analyzed by gas chromatography. GC analysis was performed with a Perkin−Elmer Autosystem. A fused silica column was employed (dimension 5 m × 0.25 mm × 0.22 μm) with SPB-1. Carrier gas: He flow at 20 psi. Volume injected: 1 μL. Program temperature used: 80 °C for 2.5 min, 10 °C/min to 150 °C and 15 °C/min to 250 °C. Injector temperature: 280 °C; FID temperature: 280 °C. Retention times: **3** 13.5 min, **5** 7.1 min,mannose 8.1 min, mannobioside **1** 13.1 min.

Determination of the K_M (4.67 mM) and v_{MAX} (0.13 mM) parameters was performed in 50 μL reaction volume with 0.25 μg/mL enzyme concentration with *p*-nitrophenol-α-D-mannoside (PNP-Man) as substrate. Seven different substrate concentrations were used (from 0.3 mM to 15 mM), with an incubation time of 20 min. Quenching was performed by adding 300 μL of 1 M carbonate buffer at pH 12. The absorbance of the *p*-nitrophenoxide released during the enzymatic reactions was measured at 400 nm and 25 °C on a UV/Vis Spectrometer (Perkin−Elmer Lambda 6).

Mannosidase inhibition studies were performed using a fixed 1.8 mM substrate (PNP-Man) concentration and variable inhibitor (**3**) concentrations in a reaction volume of 20 μL (Table 2). Enzymatic reactions were run with 2.5 μg/mL enzyme concentration in

pH 4.5 0.1 M phosphate-citrate buffer at 25 °C. After 20 min the reactions were quenched by addition of 130 μL of 1 M carbonate solution (pH 12) and the absorbance was measured at 400 nm and 25 °C on a UV/Vis Spectrometer.

Computational Methods: All calculations were performed using the MacroModel/Batchmin[21] package (version 5.5) and the AMBER* force field with the Senderowitz−Still all-atom pyranose parameters.[22] Charges were taken from the force field (all-atom charge option). Water solvation was simulated using MacroModel's generalized Born GB/SA continuum solvent model.[23] The conformational search for **3** was carried out using 10000 steps of the usage-directed MC/EM procedure. The glycosidic linkages and all the extra-annular C−C bonds were used as explicit variables during the Monte Carlo search. Extended non-bonding cut-off distances (a van der Waals cut-off of 8.0 Å and an electrostatic cut-off of 20.0 Å) were used both for the MC/EM and MC/SD calculations. The same degrees of freedom of the MC/EM searches were used in the MC/SD runs. All simulations were performed at 300 K, with a dynamic time-step of 1.5 fs and a frictional coefficient of 0.1 ps^{-1}. One Monte Carlo step was performed after each dynamic step. The average acceptance ratio was 6%. Two simulations of 5 ns each were performed starting from the lowest energy *E* and *S* conformations. Structures were sampled every 2 ps and saved for later evaluation. The interatomic distances reported in Table 1 under the MC/SD header were evaluated from $<r^{-6}>$, which was monitored during the simulation (option MDDI of Batchmin).

Acknowledgments

The project was supported by the Improving Human Potential Program under contract HPRN-CT-2002−00173 (Glycidic Scaffolds Network). Funding from the Ministry of Science and Technology of Spain (BQU2003-3550-C03), MIUR, and CNR is also acknowledged.

[1] P. Sears, C. H. Wong, *Angew. Chem.* **1999**, *111*, 2446−2471; *Angew. Chem. Int. Ed.* **1999**, *38*, 2300−2324, and references cited therein.
[2] R. Thomson, M. von Izstein, in *Carbohydrate Based Drug Discovery* (Ed.: C. H. Wong), **2004**, vol. 2, pp. 831−861.
[3] R. Horstkorte, O. T. Keppler, W. Reutter, in *Carbohydrate Based Drug Discovery* (Ed.: C. H. Wong), **2004**, vol. 2, pp. 863−873.
[4] A. Bernardi, D. Arosio, L. Manzoni, F. Micheli, A. Pasquarello, P. Seneci, *J. Org. Chem.* **2001**, *66*, 6209−6216.
[5] A. Bernardi, P. Brocca, A. Checchia, S. Sonnino, F. Zuccotto, *J. Am. Chem. Soc.* **1999**, *121*, 2032−2036.
[6] A. Bernardi, D. Arosio, S. Sonnino, *Neurochem. Res.* **2002**, *27*, 539−545, and references cited therein.
[7] A. Bernardi, D. Potenza, A. M. Capelli, A. García-Herrero, F. J. Cañada, J. Jiménez-Barbero, *Chem. Eur. J.* **2002**, *8*, 4597−4612.
[8] A. Bernardi, D. Arosio, L. Manzoni, D. Monti, H. Posteri, D. Potenza, S. Mari, J. Jimenez-Barbero, *Org. Biomol. Chem.* **2003**, *1*, 785−792.
[9] [9a] E. A. Merrit, S. Sarfaty, F. v. d. Akker, C. L′Hoir, J. A. Martial, W. G. J. Hol, *Protein Sci.* **1994**, *3*, 166−175. [9b] E. A. Merrit, S. Sarfaty, M. G. Jobling, T. Chang, R. K. Holmes, T. R. Hirst, W. G. J. Hol, *Protein Sci.* **1997**, *6*, 1516−1528. [9c] E. A. Merrit, W. G. J. Hol, *Curr. Opin. Struct. Biol.* **1995**, *5*, 165−171 and references cited therein.
[10] [10a] D. Arosio, S. Baretti, S. Cattaldo, D. Potenza, A. Bernardi, *Bioorg. Med. Chem. Lett.* **2003**, *13*, 3831−3834. [10b] A. Bernardi, D. Arosio, D. Potenza, I. Sanchez-Medina, S. Mari, F. J. Cañada, J. Jimenez-Barbero, *Chem. Eur. J.* **2004**, *10*, 4395−4406.
[11] V. V. Samoshin, V. A. Chertkov, L. P. Vatlina, E. K. Dobretsova, N. A. Simonov, L. P. Kastorsky, D. E. Gremyachinsky, H.-J. Schneider, *Tetrahedron Lett.* **1996**, *37*, 3981−3984.
[12] A. Bernardi, D. Arosio, D. Dellavecchia, F. Micheli, *Tetrahedron: Asymmetry* **1999**, *40*, 3403−3407.
[13] [13a] T. Ren, D. Liu, *Tetrahedron Lett.* **1999**, *40*, 7621−7625. [13b] R. R. Schmidt, J. Michel, *Angew. Chem. Int. Ed. Engl.* **1980**, *19*, 731−732. [13c] R. R. Schmidt, *Angew. Chem. Int. Ed. Engl.* **1986**, *25*, 212−235.
[14] W. Wang, F. Kong, *J. Org. Chem.* **1998**, *63*, 5744−5745; W. Wang, F. Kong, *Angew. Chem. Int. Ed.* **1999**, *38*, 1247−1250.
[15] R. J. Woods, A. Pathiaseril, M. R. Wormald, C. J. Edge, R. A. Dwek, *Eur. J. Biochem.* **1998**, *259*, 372−386, and references cited therein.
[16] A. Bernardi, A. Colombo, I. Sánchez-Medina, *Carbohydr. Res.* **2004**, *339*, 967−973, and references cited therein.
[17] M. R. Wormald, A. J. Petrescu, Y.-L. Pao, A. Glithero, T. Elliot, R. A. Dwek, *Chem. Rev.* **2002**, *102*, 371−386 and references cited therein.
[18] Y.-T. Li, *J. Biol. Chem.* **1967**, *242*, 5474−5480.
[19] [19a] Y. Bourne, V. Zamboni, A. Barre, W. J. Peumans, E. J. M. Van Damme, P. Rouge, *Structure* **1999**, *7*, 1473−1482. [19b] D. N. Moothoo, B. Canan, R. A. Field, J. Naismith, *Glycobiology* **1999**, *9*, 539−545. [19c] D. A. R. Sanders, D. N. Moothoo, J. Raftery, A. J. Howard, J. R. Helliwell, J. H. Naismith, *J. Mol. Biol.* **2001**, *310*, 875−884. [19d] C. A. Bewley, *Structure* **2001**, *9*, 931−940; L. C. Chang, C. A. Bewley, *J. Mol. Biol.* **2002**, *318*, 1−8. [19e] S. R. Shenoy, L. G. Barrientos, D. M. Ratner, B. R. O'Keefe, P. H. Seeberger, A. M. Gronenborn, M. R. Boyd, *Chem. Biol.* **2002**, *9*, 1109−1118. [19f] C. A. Bewley, S. Kiyonaka, I. Hamachi, *J. Mol. Biol.* **2002**, *322*, 881−889. [19g] C. N. Scanlan, R. Pantophlet, M. R. Wormald, E. O. Saphire, R. Stanfield, I. A. Wilson, H. Katinger, R. A. Dwek, P. M. Rudd, D. R. Burton, *J. Virol.* **2002**, *76*, 7306−7321.
[20] W. B. Turnbull, B. L. Precious, S. W. Homans, *J. Am. Chem. Soc.* **2004**, *126*, 1047−1054.
[21] F. Mohamadi, N. G. J. Richards, W. C. Guida, R. Liskamp, M. Lipton, C. Caufield, G. Chang, T. Hendrickson, W. C. Still, *J. Comp. Chem.* **1990**, *11*, 440−467.
[22] H. Senderowitz, W. C. Still, *J. Org. Chem.* **1997**, *62*, 1427−1438.
[23] W. C. Still, A. Tempzyk, R. Hawley, T. Hendrickson, *J. Am. Chem. Soc.* **1990**, *112*, 6127−6129.

Received July 23, 2004

